

Targeted induction of meiotic double-strand breaks reveals chromosomal domain-dependent regulation of Spo11 and interactions among potential sites of meiotic recombination

Tomoyuki Fukuda^{1,*}, Kazuto Kugou^{1,2}, Hiroyuki Sasanuma^{1,2},
Takehiko Shibata¹ and Kunihiro Ohta^{1,2}

¹Shibata Distinguished Senior Scientist Laboratory, RIKEN, 2-1 Hirosawa, Wako, Saitama 351-0198 and

²Department of Life Sciences, Graduate School of Arts and Sciences, University of Tokyo, 3-8-1 Komaba, Meguro-ku, Tokyo 153-8902, Japan

Received October 17, 2007; Revised and Accepted November 17, 2007

ABSTRACT

Meiotic recombination is initiated by programmed DNA double-strand break (DSB) formation mediated by Spo11. DSBs occur with frequency in chromosomal regions called hot domains but are seldom seen in cold domains. To obtain insights into the determinants of the distribution of meiotic DSBs, we examined the effects of inducing targeted DSBs during yeast meiosis using a UAS-directed form of Spo11 (Gal4BD-Spo11) and a meiosis-specific endonuclease, VDE (PI-SceI). Gal4BD-Spo11 cleaved its target sequence (UAS) integrated in hot domains but rarely in cold domains. However, Gal4BD-Spo11 did bind to UAS and VDE efficiently cleaved its recognition sequence in either context, suggesting that a cold domain is not a region of inaccessible or uncleavable chromosome structure. Importantly, self-association of Spo11 occurred at UAS in a hot domain but not in a cold domain, raising the possibility that Spo11 remains in an inactive intermediate state in cold domains. Integration of UAS adjacent to known DSB hotspots allowed us to detect competitive interactions among hotspots for activation. Moreover, the presence of VDE-introduced DSB repressed proximal hotspot activity, implicating DSBs themselves in interactions among hotspots. Thus, potential sites for Spo11-mediated DSB are subject to domain-specific and local competitive regulations during and after DSB formation.

INTRODUCTION

Meiosis is a specialized cell cycle that occurs during the formation of gametes. During meiosis, recombination is a key event, not only in that it acts as a source of genetic variation, but also in that it forms physical connections between homologous chromosomes known as chiasmata, which permit proper segregation of homologous chromosomes (1). Meiotic recombination is initiated by programmed DNA double-strand break (DSB) formation catalyzed by a type II topoisomerase-like protein, Spo11 (2). In addition to Spo11, several conserved and non-conserved gene products have also been revealed to be involved in meiotic DSB formation (2–5); however the precise roles of these additional factors remain unclear. Meiotic DSBs are repaired using the unbroken homologous chromatid as a template to produce alternative recombinants, non-crossovers and crossovers, the latter of which result in chiasma formation (1).

In a variety of organisms, meiotic recombination occurs non-randomly along chromosomes (6). Mainly based on studies of the yeast *Saccharomyces cerevisiae*, formation of DSB during meiosis is thought to be controlled by several factors that influence the number and position of DSBs. First, meiotic recombinations are preferentially initiated at defined sites called recombination hotspots. In hotspots, DSBs occur within a region of 50–250 bp, in which no obvious consensus sequences have been found (2,7). Most hotspots are in intergenic regions, which often harbor binding sites for transcription factors. DSB activity at some hotspots is dependent on the binding of transcriptional machinery but does not directly correlate with transcriptional activity (8,9). Hotspots are also

*To whom correspondence should be addressed. Tel: +81 (0) 48 467 9277; Fax: +81 (0) 48 462 4691; Email: tfukuda@riken.jp
Correspondence may also be addressed to Kunihiro Ohta. Tel: +81 (0) 3 5465 8834; Fax: +81 (0) 3 5465 8834; Email: kohta@bio.c.u-tokyo.ac.jp

frequently found at ectopic insertions of external sequence (10–12). A common feature of hotspots is that they are located in accessible regions of chromatin that are hypersensitive to DNaseI and micrococcal nuclease (MNase) (13–15). Additionally, neighboring hotspots appear to interact: insertion of a hotspot near a pre-existing hotspot reduces the activity of both hotspots, and deletion of a hotspot can stimulate a new site of DSB (11,12,16).

Chromosome- or genome-wide analyses of meiotic DSBs have also revealed that DSBs are likely to occur preferentially in chromatin loops, away from DNA-axis associations mediated by cohesins and axial-element (AE) proteins (17,18). In addition, at least in *rad50S* or *sae2A* mutant, a large fraction of hotspots cluster in 50–100 kb domains (hot domains) and few DSBs occur in domains near telomeric or centromeric regions (cold domains) (19,20). The locations of many hotspots correlate with regions with high GC content (6,18). These features of higher-order chromosome structure appears to be more important to DSB formation than local structure of open chromatin, as open chromatin sites can be found in cold domains (21). Moreover, the frequency of DSB formation in an integrated hotspot sequence depends on the broader context, i.e. insertion in a hot or cold domain, even when the hotspot sequence has a constitutively open chromatin configuration (21,22). It is to be noted that some of the features of the chromosomal distribution of DSBs are likely to be exaggerated since those have been revealed using *rad50S* or *sae2A* mutants, which accumulate unprocessed DSBs but have reductions in DSBs at particular regions (23).

Studies with Spo11 fused to the DNA-binding domain of Gal4 (Gal4BD-Spo11) have provided important insights into the control of DSBs. Gal4BD-Spo11 can stimulate novel DSBs at Gal4-binding sequences in normally cold regions, raising the possibility that DNA binding by Spo11 is a primary determinant of DSB sites (24). However, genome-wide mapping analysis recently revealed that the distribution of DSB sites formed by Gal4BD-Spo11 does not necessarily correspond to that of the binding sites of Gal4BD-Spo11, indicating that binding of Spo11 *per se* is not sufficient for a DSB (25).

In spite of the accumulating knowledge on the topic, the molecular mechanisms governing the distribution of DSBs remain to be elucidated. Control of the amount and positions of DSBs appears to be important, because reduction of *in vivo* activity of Spo11 decreases spore viability in yeast and because occurrence of cross-overs around centromeric or telomeric regions is deleterious to accurate chromosome transmission (26–28). In this study, to obtain insights into the molecular basis of meiotic DSB distribution, we induced formation of site-specific DSBs using Gal4BD-Spo11 and an intein-encoded nuclease, VDE (also called PI-SceI). VDE is a member of the homing endonuclease protein family and in a Spo11-independent manner, can generate a DSB at the VDE-recognition sequence (VRS) during meiosis of *S. cerevisiae* (29,30). Integration of the Gal4-binding sequence and VRS enables tethering the endonuclease to a chromosomal site of interest. Using this system,

we uncovered multiple pathways for spatial control of meiotic DSB formation, by means of which a limited number of DSBs are formed in distinct chromosomal domains.

MATERIALS AND METHODS

Strains and culture conditions

Yeast strains used in this study are of the SK1 background (31) and are listed in Table S1 in the Supplementary Data. Strains were constructed via standard genetic crosses, transformation and other genetic procedures (32). The *VMA1-105* allele is a complete deletion of the *VMA1* intein [*VMA1*(–)] and the *VMA1* allele contains the *VMA1* intein [*VMA1*(+)] (33). The plasmids pTF101 (34) or pTF100 (see below) were used for integration of sequences containing VRS or the promoter region of the *GAL2* gene (UAS), respectively. Sequences of primers used for integration of VRS or UAS are listed in Table S2 in the Supplementary Data. Gal4BD-Spo11, Gal4BD-Spo11-Flag and Spo11-Flag were expressed under the *ADHI* promoter at the *TRP1* gene locus using strains with a complete deletion of the authentic *SPO11* gene. Wild-type Spo11 was expressed from the authentic gene. The alleles expressing Gal4BD-Spo11 and Gal4BD-Spo11-Flag were derived from ORD5806 (24) and YHS900 (35), respectively. For expression of Spo11-Flag, integration plasmid harboring *ADHI*-promoter-fused *GAL4BD-SPO11-FLAG* was replaced by the *ADHI*-promoter-fused *SPO11-FLAG* fragment from pAUS (35). The resultant plasmid was integrated into the *TRP1* gene locus. To examine genetic rearrangement of genes around *HIS3*, the neighboring genes *MCA1* and *FMP38* were replaced with the *CgLEU2* and *CgURA3* gene, respectively (36), with primers described previously (34). All integrations and gene disruptions were confirmed by PCR or Southern blot analysis.

Synchronous meiosis was performed essentially as described previously (37). Strains were grown in presporulation medium, SPS (0.5% yeast extract, 1% peptone, 0.17% yeast nitrogen base without ammonium sulfate and amino acids, 0.05 M potassium phthalate, 1% potassium acetate and 0.5% ammonium sulfate, pH 5.0), and then shifted into sporulation medium (SPM, 1% potassium acetate). Cells were cultured with vigorous aeration at 30°C.

Plasmids

The plasmid pTF100 was created such that the promoter region of the *GAL2* gene was placed on both sides of the *URA3* gene in the pBluescript SK vector (Stratagene). The primer pairs TFO1 (5'-CTA GTC TAG ATG GTA CGA CAT GTA TTC CAG ATT CGG AAA GCT TCC TTC CGG AAT G-3'), TFO2 (5'-CTA GCC CGG GGT TCG GAG TGA TCC GCC CCG ATA CT-3'), TFO3 (5'-CTA GCC CGG GAT TCG GAA AGC TTC CTT CCG GAA TG-3') and TFO4 (5'-CTA GCT CGA GTA GTA CGC TTC ATA ATT GGT GTT CGG AGT GAT CCG CCC CGA TAC T-3') were used for amplification of the upstream region of *GAL2* using genomic DNA

as a template. The PCR fragments were cloned into XhoI–XbaI interval of pBluescript SK, followed by the insertion of the *URA3* gene at the SmaI site. The resultant plasmid, pTF100, was used as a template for amplification of the UAS–*URA3*–UAS cassette using a primer pair containing 5'-TGG TAC GAC ATG TAT TCC AG-3' and 5'-TAG-TAC GCT TCA TAA TTG GT-3' at each 3'-terminal, which can also be used to amplify the VRS–*URA3*–VRS cassette using pTF101 as a template (34).

Chromatin preparation and Southern blotting

Preparation of crude chromatin fractions from meiotic yeast cells and treatment of chromatin with MNase were performed as described (38). For Southern blot analysis, genomic DNA isolated from each sample was digested with the appropriate restriction enzymes, separated by agarose gel electrophoresis and transferred to a positively charged membrane (GE Healthcare). Restriction enzymes used for detections of DSB signals were as follows: HpaI for *HIS3*; BglIII for *YCL056C*, *HIS4*, the *YCR048W* hotspot and *YCR099C*; XhoI for *YCP4*; PstI for the *GATI* hotspot; and AseI for the *CYS3* hotspot. Probes were prepared by random priming of DNA fragments of appropriate PCR-amplified products. The sequences of the PCR primers used for generating probes are listed in Table S2 in the Supplementary Data. The membranes were hybridized according to Church and Gilbert (39). Pulsed-field gels were run, blotted and hybridized as described (21).

Chromatin immunoprecipitation (ChIP) assay

ChIP was performed essentially as described (35). Aliquots of premeiotic (0 h) or meiotic (3 h) cells were fixed in 1% formaldehyde for 15 min at room temperature, quenched for 5 min with glycine and lysed with zirconia beads using a Multibeads-Shocker (Yasui Kikai). Samples were sonicated to shear chromatin, and then immunoprecipitations were carried out with anti-Flag antibody (Sigma) bound to protein G or protein A-coated Dynabeads (Invitrogen). Recovered DNA was subjected to quantitative PCR analysis in real-time using an ABI 7300 (Applied Biosystems) with SYBR Premix ExTaq and ROX-dye (Takara) following the manufacturer's protocol. The primer pairs used in the assay were as follows: for TEL, 5'-GCG TAA CAA AGC CAT AAT GCC TCC-3' and 5'-CTC GTT AGG ATC ACG TTC GAA TCC-3'; for UAS, 5'-CGG AAA GCT TCC TTC CGG AAT GGC-3' and 5'-TCG TCC AAG GCA CAT GGA CCC CTG-3'; for *HIS4*, 5'-GGA AAG GTG ATG CTA AGC CAA AG-3' and 5'-TCG ATG ATC GGA TTG ACT AAA TGC-3'; and for CWH43, 5'-TAC CAT GGG GAA CAG GGA TCT AAC-3' and 5'-CTG GAG AGG GCA ATA AAT GAT GCG-3'. Sequences for GAL2 primer pairs were as described (35). The amounts of immunoprecipitated DNA (IP) and whole-cell extract DNA (WCE) were measured and compared to a standard sample of yeast genomic DNA.

Tetrad analysis

For tetrad analysis, parental haploid cells were mated on YPD plates for 8 h, then transferred to sporulation plates (1% potassium acetate). After 2–3 days at 30°C, spores were dissected and incubated on YPD for 2–3 days at 30°C, followed by replica plating to the plates containing the appropriate combination of amino acids. To assess the frequency of VDE-initiated recombination, we prepared VRS-integrated haploid strain and *URA3*-integrated haploid strain for each gene locus using pTF101 and pTF102, respectively, as previously described (34). Unidirectional recombination rates were measured based on the segregation pattern of *URA3*. For the 4:0 and 3:1 tetrads, the frequency of recombination was calculated on the basis of two and one events per two possible recombination events, respectively.

RESULTS

Gal4BD-Spo11-initiated DSB and recombination at sites of UAS integration

To study the regulation governing the distribution of meiotic DSBs, we utilized DSB targeting using Gal4BD-Spo11 or VDE during yeast meiosis. We recently developed a PCR-based integration method that can be used to introduce the 200-bp sequence containing the VRS into the yeast genome repeatedly (34). This method enables us to induce VDE-initiated meiotic DSB and recombination at any chromosomal position of interest. We have now extended this approach to the targeting of Gal4BD-Spo11. The strategy, as outlined in Figure S1 in the Supplementary Data, is the same as that used for the integration of the VRS (34). Using this method, 260 bp of promoter region of the *GAL2* gene harboring four upstream activation sequences (UASs), which are target sites of Gal4 (24), can be introduced into yeast chromosomes. Hereafter, we refer these 200-bp and 260-bp sequences as VRS and UAS, respectively.

We first introduced UAS into the *HIS3* gene locus and examined induction of meiotic DSBs in *sae2Δ* strains, which enabled us to detect DSBs formed by Spo11, as the DSBs cannot be repaired in the background (40,41). Southern blot analysis revealed that Gal4BD-Spo11 caused meiotic DSBs (7.4% at 9 h) at sites of integration of UAS (Figure 1A). The formation of DSB depends on the UAS integration and on expression of Gal4BD-Spo11 (Figure 1A). Subsequently, recombination was also examined by measuring the genetic distance between flanking marker genes (Figure 1B). In the *GAL4BD-SPO11* strain, an increase in the genetic distance between markers indicated that UAS integration led to a higher frequency of crossovers (Figure 1B). Thus, introduction of UAS can induce meiotic DSB and recombination accompanied by frequent crossovers, a phenomenon common to endogenous hotspots.

Ectopic insertion of external sequences into chromosomes sometimes creates an open chromatin site, which is suitable for meiotic DSB formation (10–12,42). We next explored chromatin structure around the integrated UAS

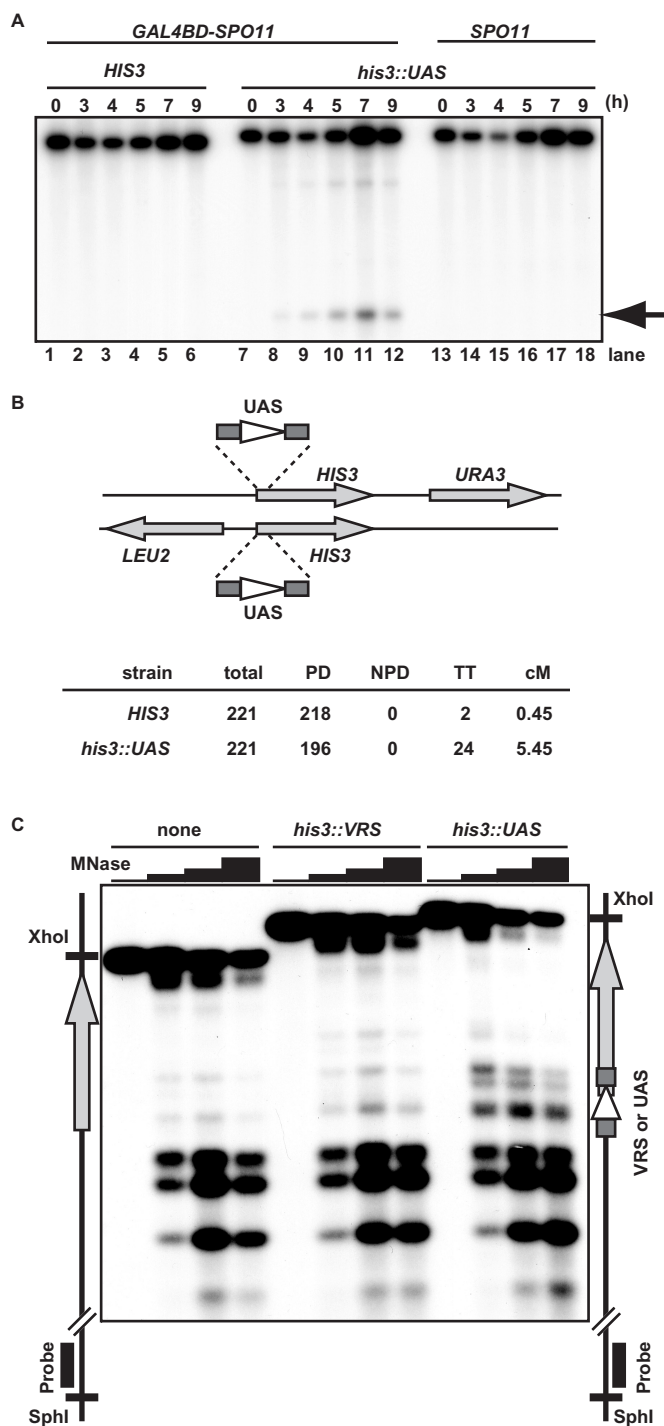


Figure 1. Induction of targeted recombination by UAS integration. (A) Genomic DNA was purified from synchronous meiotic cells at the indicated times after incubation in sporulation medium (SPM) and was subjected to Southern blot analysis using a probe for the region around *HIS3* after *HpaI* digestion. UAS was introduced at the *HIS3* gene locus (*his3::UAS*) in *sae2Δ* strains expressing Gal4BD-Spo11 or Spo11. The arrow indicates the UAS integration site. Lanes 1–6, strain TFY011; lanes 7–12, strain TFY203; lanes 13–18, strain TFY 225. (B) In the *GAL4BD-SPO11* strain, the marker genes *URA3* and *LEU2* are integrated 3.0 and 3.6 kb away from UAS insertion site, respectively. Parental ditype (PD), tetra type (TT) and nonparental ditype (NPD) asci were identified with respect to the markers. For strains without (*HIS3*) or with (*his3::UAS*) integration of UAS, the genetic distances between the markers are expressed in terms of centimorgans (cM),

or VRS by indirect end-labeling analysis of MNase-digested chromatin. Figure 1C shows positions of individual nucleosomes and nuclease-sensitive sites around *HIS3* in the presence and absence of an integrated element. Relatively strong and discrete sites of MNase sensitivity were specifically observed at the inserted UAS but little sensitivity was observed at the VRS (Figure 1C). It is likely that *cis*-acting element(s) in UAS function(s) to form an open chromatin configuration, because the authentic *GAL2* promoter also displays an open chromatin configuration (24). Although DSBs were not observed on the UAS integrated at *HIS3* in the *SPO11* strain (Figure 1A), it should be noted that the UAS insertion provides an open chromatin structure, a potential site for meiotic DSB (See below).

Gal4BD-Spo11 induces DSBs at UASs integrated in hot domains but rarely in cold domains

Robine *et al.* (25) recently reported that binding of Gal4BD-Spo11 *per se* does not necessarily produce DSBs and that the frequency of occurrence of DSBs at a Gal4-binding site is influenced by the surrounding chromosomal context. As described above, DSB hotspots are concentrated in hot domains and rarely observed in cold domains. To explore a domain effect on targeted DSB formation by Gal4BD-Spo11, we chose six gene loci in chromosome III, two of which are in a hot domain and four of which are in a cold domain (Figure 2A). UAS was integrated in the open reading frame region of each gene with the exception of *YCR099C*, where UAS was inserted 1.2-kb downstream of the stop codon. In cells harboring UAS at *HIS4* or *YCR048W*, which are within a hot domain, DSBs were frequently observed at the UAS integration site (Figure 2B). In contrast, little or no DSB signal was detected at the UAS integrated in *CWH43*, *YCP4* or *YCR099C*, each of which is located in a cold domain (Figure 2B). Significant levels of DSBs were detected at the UAS inserted at *YCL056C* in a cold domain, but the frequency was smaller than what was observed for UAS insertions in hot domains (Figure 2B and C). Thus, it appears that Gal4BD-Spo11 can form DSBs at UASs integrated in hot domains but less effectively at those in cold domains.

Since UAS integration results in an open chromatin structure (Figure 1C), creating a potential site for DSB formation, we next asked if wild-type Spo11 could introduce meiotic DSBs at sites of UAS integration. As expected, in cells expressing Spo11, DSBs were formed at UASs inserted in a hot domain, but the effect was less robust than what was observed in strains expressing

calculated using the following formula: $cM = 100 (TT + 6NPD) / (PD + TT + NPD)$. The *HIS* or *his3::UAS* strain was obtained by mating TFY179 and TFY181, or TFY180 and TFY182, respectively. (C) Meiotic chromatin (4h) was purified from *SPO11* cells without (none, strain MJL1720), or with integration of VRS (*his3::VRS*, strain TFY236) or UAS (*his3::UAS*, strain TFY237) at the *HIS3* gene. Each chromatin sample was treated with 0, 5, 10 or 20 U/ml of MNase. MNase-sensitive sites were detected by indirect end labeling using a probe for the sequence adjacent to the *SphI* site. The vertical gray arrows indicate the positions of the coding region of *HIS3*.

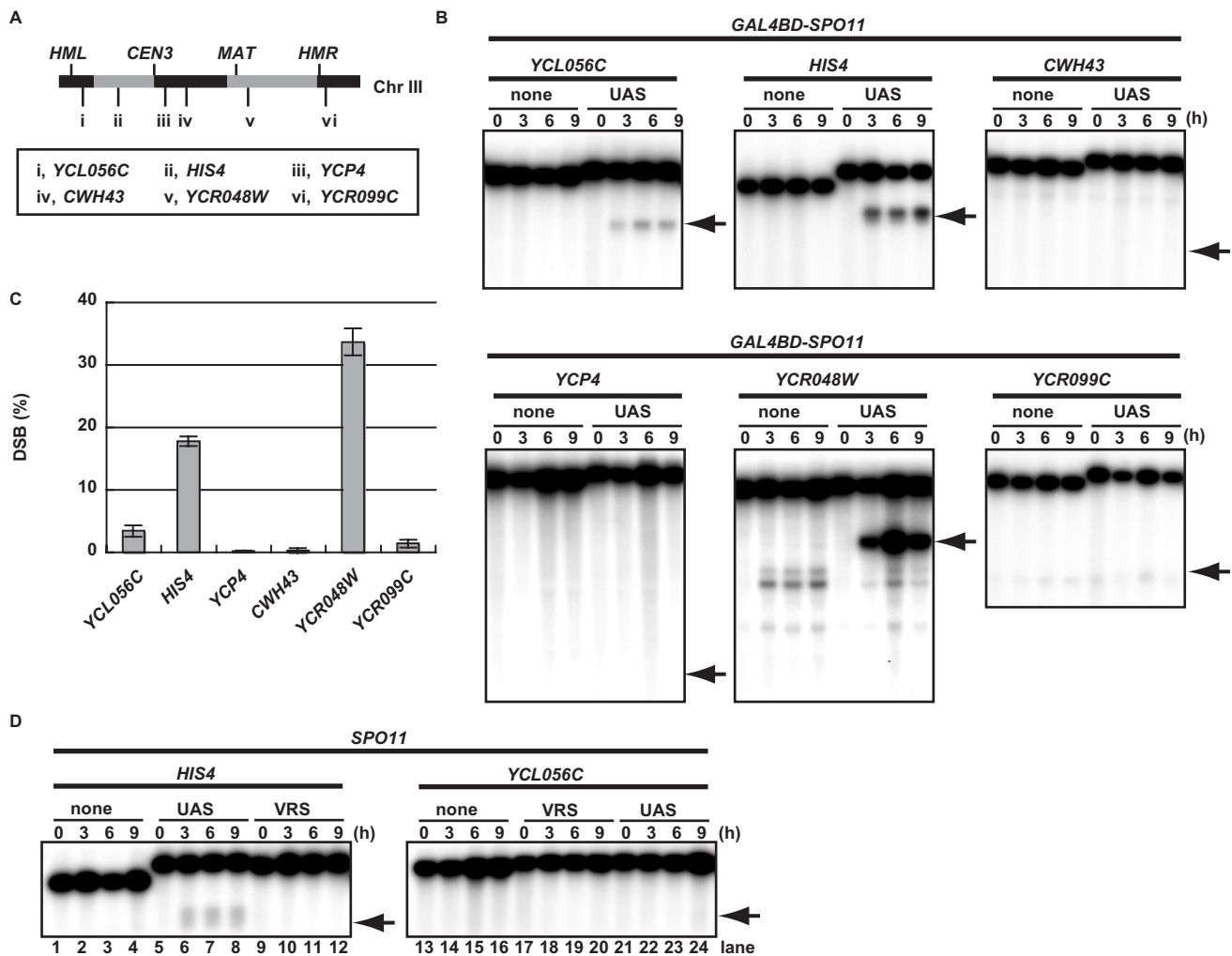


Figure 2. Domain effect on targeted DSB formation by UAS or VRS integration. (A) Six loci (i–vi) on chromosome III are indicated. Chromosomal domains as classified by Baudat and Nicolas (19) are shown, with hot domains in gray and cold domains in black. (B) Southern blot analyses were performed as described for Figure 1A on each gene locus from cells with (UAS) or without (none) integration of UAS at the sites indicated by arrows. Using TFY011 (*GAL4BD-SPO11 sae2Δ*) as a parental strain, strains harboring UAS at each gene locus were constructed and examined. For *YCL056C*, strain TFY255; for *HIS4*, strain TFY256; for *CWH43*, strain TFY258; for *YCP4*, strain TFY257; for *YCR048W*, strain TFY259; for *YCR099C*, strain TFY261. (C) Quantification of results obtained in (B). For each locus, the signal from the integration site at 6 h is represented as a mean with standard deviation from at least three independent cultures. (D) Southern blot analyses were performed on cells without (none) or with integration of VRS or UAS at each gene locus. The arrows indicate integration sites. All strains were *SPO11* with a *sae2Δ* mutation and did not express VDE. Lanes 1–4 and 13–16, strain TFY372; lanes 5–8, strain TFY500; lanes 9–12, strain TFY501; lanes 17–20, strain TFY507; lanes 21–24, strain TFY506.

Gal4BD-Spo11 (*HIS4*, Figure 2D; *YCR048W*, Figure 4A; *CYS3*, Figure S2 in the Supplementary Data). In contrast, Spo11-mediated DSBs were not observed when UAS was inserted in a cold domain (*YCL056C*, Figure 2D). Thus, we can conclude that UAS-derived open chromatin sites are sufficient to induce meiotic DSBs in a hot domain. Moreover, forcible recruitment of Spo11 to a UAS via fusion with Gal4BD further increases the frequency of DSBs in hot domains but can overcome the cold nature of a domain only to a very limited extent.

Meiotically induced self-association of Spo11 occurs in a hot domain but not in a cold domain

To explore possible causes of the domain effect on DSB formation, we assessed chromosome accessibility and

cleavability at each of the loci we tested. First, ChIP assays revealed that Gal4BD-Spo11 bound the UAS to a similar extent at each integration site (Figure 3A). Thus, the data show that the domain effect cannot simply be attributed to accessibility to Gal4BD-Spo11, consistent with the results of Robine *et al.* (25). Second, we examined the frequency of VDE-produced DSBs at VRSs inserted in the same loci. Diploid strains heterozygous for the VRS-inserted allele and an *URA3*-inserted allele at each gene locus were prepared and the frequency of DSB formation in each was measured by determining the unidirectional gene conversion rate of the VRS-inserted allele to the *URA3*-inserted allele. As shown in Figure 3B, VDE efficiently induced recombination regardless of location, indicating that cold domains are also accessible to VDE

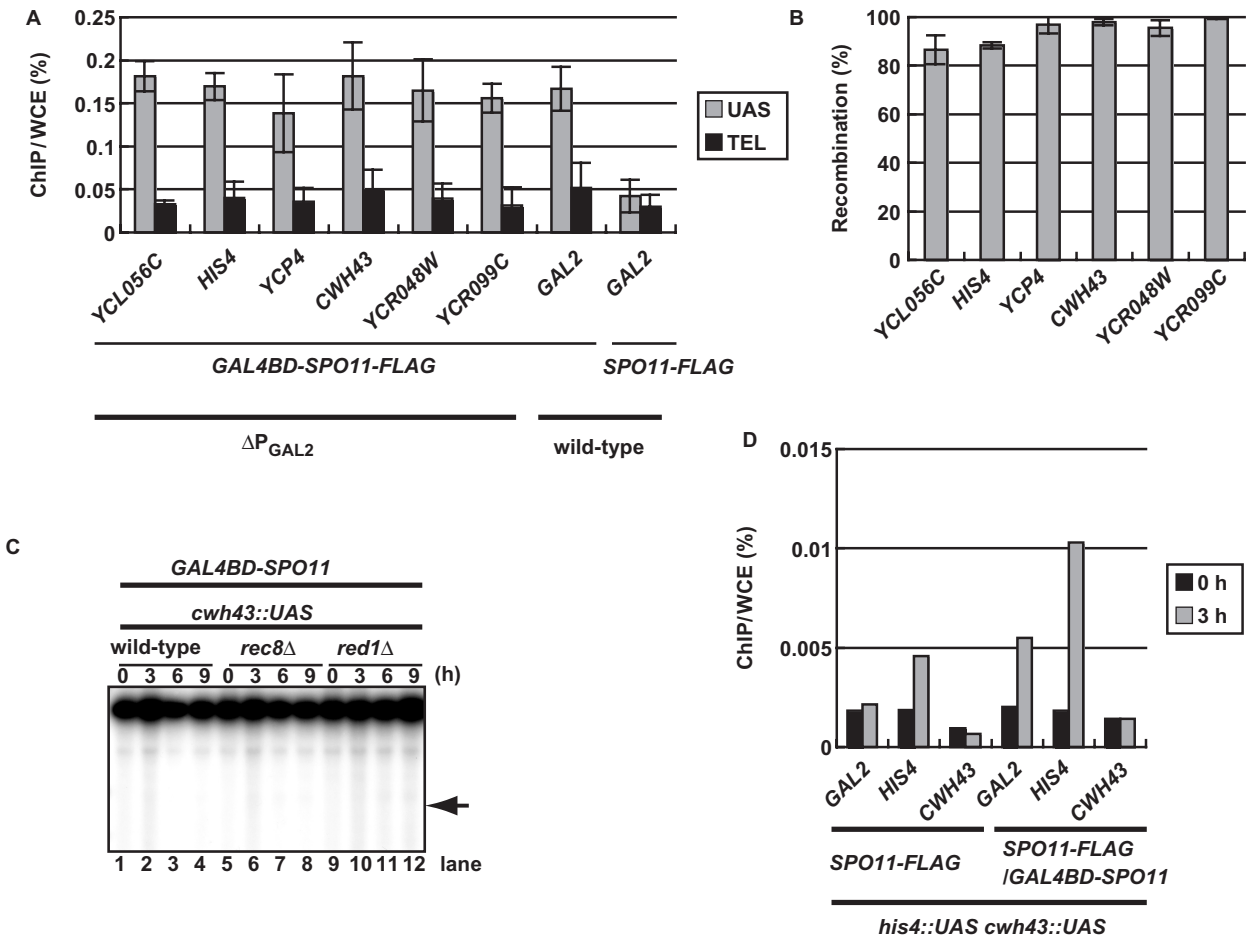


Figure 3. Exploring the causes of the domain effect of meiotic DSB. (A) Chromatin binding of Gal4BD-Spo11 at UAS inserted in each gene locus. In the UAS-inserted cells (ΔP_{GAL2}), authentic UAS at the upstream region of *GAL2* is deleted so that they should contain a single copy of UAS only at the insertion site, whereas non-inserted cells (wild-type) have UAS only at the *GAL2* site. Gal4BD-Spo11-Flag and Spo11-Flag were expressed during both mitosis and meiosis, as they are under the control of the *ADH1* promoter. For premeiotic cells (0 h), ChIPs were performed as described in Materials and Methods section. DNA purified from the immunoprecipitations was subjected to quantitative real-time PCR using primers specific to UAS or the telomere region of chromosome VI (TEL). Error bars denote the standard deviation among three independent experiments. The cells used were *GAL4BD-SPO11-FLAG* strains harboring UAS at *YCL056C* (strain TFY277), *HIS4* (strain TFY278), *YCP4* (strain TFY279), *CWH43* (strain TFY280), *YCR048W* (strain TFY281), or *YCR099C* (strain TFY282), *GAL4BD-SPO11-FLAG* strain without UAS-integration (strain TFY326) and *SPO11-FLAG* strain without UAS-integration (strain TFY325). (B) Frequency of VDE-induced recombination at the indicated sites. For each gene locus, strains heterozygous for the VRS-integrated allele (derivatives of strain TFY286) and the *URA3*-integrated allele (derivatives of strain YOC3685) were constructed. Recombination frequency was calculated based on the segregation pattern of *URA3* for at least 44 four-spore-viable tetrads per one experiment. Error bars denote the standard deviation among three independent experiments. (C) A deletion of a gene encoding a chromosome core protein was introduced into the *GAL4BD-SPO11 sae2Δ* strain that contains UAS integration at the *CWH43* gene locus indicated by the arrow. Southern blot analysis was performed as in Figure 2B. Lanes 1–4, strain TFY081; lanes 5–8, strain TFY082; lanes 9–12, strain TFY083. (D) Meiotic association of Spo11-Flag with UAS mediated by Gal4BD-Spo11. ChIP was performed on premeiotic (0 h) and meiotic (3 h) cells. All forms of Spo11 were expressed during both mitosis and meiosis, as they are under the control of the *ADH1* promoter. The strains have three copies of the *GAL2* promoter, two of which are integrated at *HIS4* and *CWH43* and the other of which is at the authentic site (*GAL2*). Binding of Spo11-Flag to each UAS in the absence (strain TFY091) or presence (strain TFY092) of Gal4BD-Spo11 was examined with primers specific to sequences adjacent to each UAS.

and that cold domains are not regions of uncleavable chromosome structure. Next, we tested whether chromosome core components have a role in the domain effect as the distribution of meiotic DSBs appears to be influenced by that of chromosome axis and chromatin loops (17,18,20). DSB formation by Gal4BD-Spo11 at the *CWH43* locus, which is located in a cold domain, was analyzed in the absence of the meiotic cohesin component, Rec8, or the AE protein, Red1, both of which are main components of the chromosome axis during meiosis

(18,43,44). We found that DSB formation was not restored at the UAS integrated at *CWH43* in either mutant strain (Figure 3C), suggesting that the domain effect cannot be attributed to differences in chromosome structure mediated by these proteins.

It has been revealed that association between Spo11 occurs during meiosis in a genetically controlled manner (35). In a strain co-expressing Gal4BD-Spo11 and Spo11-Flag, self-association of Spo11 can be detected as recruitment of Spo11-Flag to a UAS site via its interaction

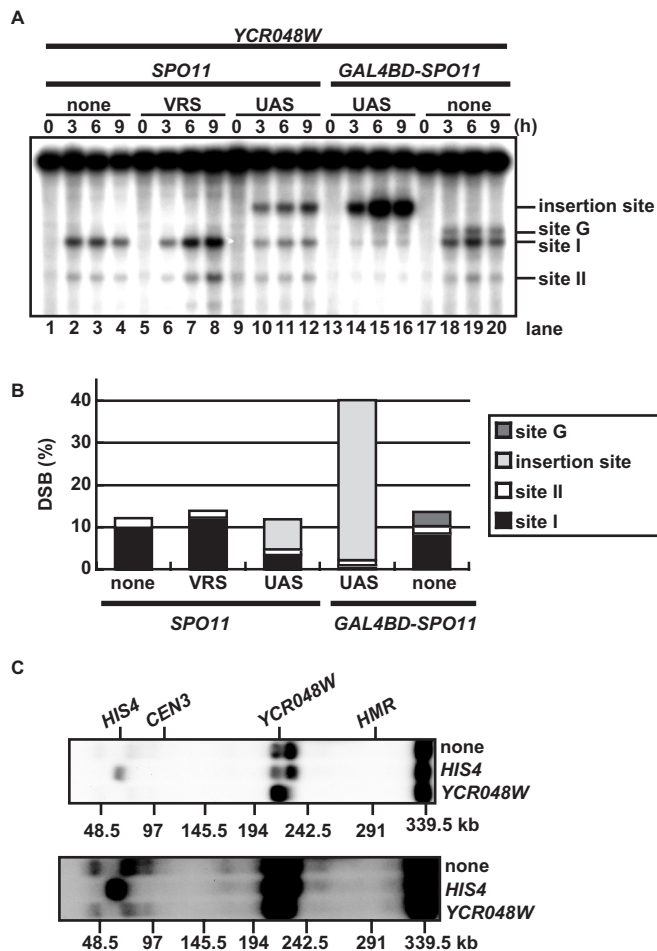


Figure 4. Repression of hotspot activity by UAS integration. (A) Southern blot analysis was performed on strains expressing Spo11 or Gal4BD-Spo11 without (none) or with integration of UAS or VRS at the *YCR048W* gene locus. All strains are *sae2Δ* background. The insertion site, two prominent natural hotspots (site I and II), and a Gal4BD-Spo11-dependent hotspot (site G) are indicated. Lanes 1–4, strain TFY372; lanes 5–8, strain TFY505; lanes 9–12, strain TFY504; lanes 13–16, strain TFY259; lanes 17–20, strain TFY011. (B) Quantification of results obtained in (A). The amounts of DSB signal at 6 h are represented as a histogram. (C) Pulsed-field gels of undigested DNA from meiotic cells. DSBs along chromosome III were detected by Southern blot analysis with a probe specific to the end of the left arm. *GAL4BD-SPO11 sae2Δ* strains without (none, strain TFY011) or with the UAS insertion at *YCR048W* (strain TFY259) or *HIS4* (strain TFY256) are shown. A longer exposure of the blot is also shown (lower panel).

with Gal4BD-Spo11 (35). Using this system, we examined whether Spo11 self-interaction occurs at UASs located in the *CWH43*, *HIS4* and *GAL2* loci. As expected, in a strain co-expressing Spo11-Flag and Gal4BD-Spo11, Spo11-Flag was recruited onto the UASs of *HIS4* and *GAL2* during meiosis as observed by ChIP (Figure 3D). However, Spo11-Flag was not detected on the UAS integrated at *CWH43* (Figure 3D). These data suggest that meiotic self-association of Spo11 does not occur in a domain where Gal4BD-Spo11 cannot introduce meiotic DSBs. Taken together, our data raise the possibility that although cold domains are accessible and potentially

cleavable, Spo11 remains in an inactive state and does not self-associate in cold domains.

Effects of UAS insertion near meiotic DSB hotspots

Hotspots that are present in close proximity to one another have been observed to compete for meiotic DSB formation in some chromosome contexts but not in others (11,12,16,45). To systematically study interactions among hotspots, we constructed strains harboring UAS or VRS proximal to well-known hotspots and then assessed DSB formation around the hotspots. Experiments were performed using the *VMA1(-)* strain, which does not express VDE. Around the *YCR048W* locus, two major hotspots (Figure 4A, sites I and II) exist and an additional hotspot (Figure 4A, site G) appears when Gal4BD-Spo11 is expressed (24). We constructed strains in which UAS or VRS was integrated in the *YCR048W* gene about 1.3 kb away from the site I hotspot, and examined DSBs in the strains by Southern blot analysis (Figure 4A). In the *SPO11* strain, meiotic DSBs were observed at the UAS integration site (Figure 4A, lanes 9–12), probably due to the open chromatin structure created by UAS integration. We also noted a concomitant reduction in DSB signals at natural *YCR048W* hotspots (Figure 4A and B). By contrast, integration of VRS did not form DSBs at the integration site, nor did it reduce the frequency of formation of DSBs at neighboring hotspots (Figure 4A, lanes 5–9). Therefore, the lower level of hotspot activity near the UAS integration site is not a simple consequence of an artificial sequence interruption. Instead, it is more likely that competitive interactions among DSB sites occur around the UAS insertion. This notion is consistent with the observation that the total amount of DSBs in the 11-kb region around *YCR048W* appears to be nearly constant (Figure 4B), implying competition for DSB capacity in the region. Furthermore, in the *GAL4BD-SPO11* strain, the integration of UAS resulted in more frequent DSB formation at the UAS, with DSBs at native hotspots much less frequent (Figure 4A, lanes 13–16). In contrast to what was observed for the *SPO11* strain, in the UAS-integrated *GAL4BD-SPO11* strain, the total DSBs within the 11-kb interval was much higher than in the strain without integration (Figure 4B). This suggests that Gal4BD-Spo11 allows recruitment of the DSB formation machinery to the integrated UAS more efficiently than wild-type Spo11, increasing the capacity for DSBs in this interval. This explanation is supported by chromosome-wide detection of DSBs, wherein DSBs were frequently induced at the UAS by Gal4BD-Spo11 and caused long-range repression within a >30-kb interval, such that the total number of DSBs was kept constant (Figure 4C).

We also introduced UAS or VRS into the *CYS3* hotspot, where two major break sites can be detected. As shown in Figure S2, the results were similar to what was found for insertions at *YCR048W*. UAS insertion caused meiotic DSBs at the site and reduced nearby hotspot activity, whereas introduction of VRS at the same site had no effect. Although the UAS insertion in the *SPO11* strain caused little alteration in the total amount

of DSBs around *CYS3*, Gal4BD-Spo11 stimulated DSBs at the inserted UAS at levels higher than the innate permissible level for the interval.

In contrast to *YCR048W* and *CYS3*, a different feature was observed around an UAS integration at the *GATI* hotspot on chromosome VI. When UAS was introduced 0.3 kb away from the *GATI* hotspot in the *SPO11* strain, hotspot activity was severely repressed and DSBs were not detected at the inserted UAS (Figure 5B, lanes 1–8). Hotspot activity gradually increased as the UAS was inserted further from the hotspot, whereas DSB formation at the inserted UAS remained at lower than detectable levels (Figure 5B and C). Insertion of VRS at the same sites neither repressed DSB formation at the *GATI* hotspot nor caused DSBs at the insertion site (Figure 5B, lanes 17–32), indicating that inactivation of the *GATI* hotspot by the UAS insertion was not simply due to an interruption of the DNA sequence around *GATI*. Thus, in this region, local UAS integration *per se* prevents nearby meiotic DSB formation. We further examined the effect of UAS integration around *GATI* in a strain expressing Gal4BD-Spo11. In the strain, DSBs were observed at the integrated UAS (Figure 5B, lanes 33–48) and *GATI* hotspot activity was slightly higher in comparison with the *SPO11* strain harboring UAS at the same site (Figure 5C). Thus, forced recruitment of the DSB formation machinery to the UAS may enhance the capacity to form DSBs at this region and thus overcome the inhibitory effects of the UAS insertion.

Next, we investigated possible causes of the inhibitory effect of UAS at *GATI*. Binding of the transcription machinery affects some meiotic DSBs (8,9). To examine whether the binding of authentic Gal4 to UAS prevents *GATI* hotspot activity, we deleted the *GAL4* gene and then assessed DSB formation around *GATI*. As shown in Figure 5D, a *gal4Δ* mutation did not restore *GATI* hotspot activity in the UAS-inserted strains, indicating that prevention of DSB formation is not due to binding of Gal4 to the UAS.

We then examined the chromatin configuration around the *GATI* gene. As observed at the *HIS3* gene locus, UAS insertions were associated with open chromatin (Figure 5E, arrowheads) whereas insertions of VRS were not. However, the chromatin configuration near the DSB site was independent of insertion, implying that prevention of hotspot activity by UAS integration is not attributed to the alteration in chromatin configuration at the *GATI* hotspot. These data raise the possibility that two neighboring open chromatin sites (i.e. potential sites of meiotic DSB formation) compete for the DSB formation machinery, leading to reduced activation at both sites (See Discussion section).

VDE-mediated DSB formation reduces proximal hotspot activity

As shown above, an UAS insertion near *GATI* hotspot repressed hotspot activity without inducing DSB formation at the UAS, implying that interactions among hotspots may occur before or during DSB formation. To examine whether a DSB itself can affect nearby

DSB formation, we next tested the effects of VDE-mediated DSBs on hotspot activity. We integrated VRS around the *GATI* hotspot in a *VMAI(+)* strain that expresses VDE. As shown in Figure 6A, VDE-mediated DSBs were induced at the inserted VRS site during meiosis. Parental bands and VDE-produced DSB fragments gradually disappeared at later time points probably because VDE efficiently cleaved all chromatids and eliminated intact templates for recombinational repair, resulting in continuous DSB end resection. DSB formation at the *GATI* hotspot was severely impaired when VDE-mediated DSBs occurred at sites located 0.3, 1.3 or 2.3 kb away from the hotspot (Figure 6A). The reduction of *GATI* hotspot activity was also seen in strains in which VRS was integrated more than 10 kb away from the hotspot, and DSB formation was partially restored when VRS was inserted 19 kb away from the hotspot (Figure 6A and B). Quantification results indicate that DSBs at the hotspot are reduced more profoundly than parental signals, suggesting that the DSB reductions were not simply due to the loss of chromosome by resection (Figure 6B).

Similarly, reduction in hotspot activity was also observed at the *YCR048W* hotspot when VDE-mediated DSBs were introduced proximally (Figure 6C and D). Figures 4A and 5B show that the VRS insertion itself does not affect hotspot activities, indicating that the observed reductions are due to VDE-mediated DSBs. Moreover, *VMAI(+)* strains harboring VRS around *GATI* displayed normal DSB formation at the *YCR048W* hotspot and *vice versa* (data not shown), indicating that the influence of VDE-mediated DSB is local or regional. Thus, DSB formation at one site appears to prevent nearby DSB formation by Spo11 over regions of ~20 kb in length.

To study inhibition caused by VDE-mediated DSBs at the *GATI* hotspot in more detail, we prepared a diploid strain in which part of the *BUD27* gene, which is upstream of *GATI*, was replaced by a marker gene on one chromosome (Figure 7A, *bud27::L*) but not the other. This replacement enables us to detect each chromosome separately by Southern blot analysis with probes that recognize the *BUD27* region that is present only on one chromosome (Figure 7A, M probe) or recognize the marker gene (Figure 7A, P probe). We introduced VRS 2.3 kb away from the *GATI* hotspot on one homolog but not on the other. These strains are useful to examine the effect of VDE-mediated DSB on the cleaved chromosome (*cis* effect) and on the other intact homologous chromosome (*trans* effect). Southern blot analysis revealed that replacement of a part of *BUD27* does not affect hotspot activity on either chromosome (Figure 7B, lanes 1–6 and 19–24). As expected, Spo11-mediated DSBs at the *GATI* hotspot were severely reduced on the VDE-cleaved chromosome (Figure 7B, lanes 7–12 and 31–36). Interestingly, a significant reduction in DSB formation at the hotspot was observed on the non-cleaved homologous chromosome (Figure 7B lanes 13–18 and 25–30; Figure 7C), implying a *trans* effect. Thus, the number of meiotic DSBs in each hot region may be regulated by at least two repression mechanisms, competition for

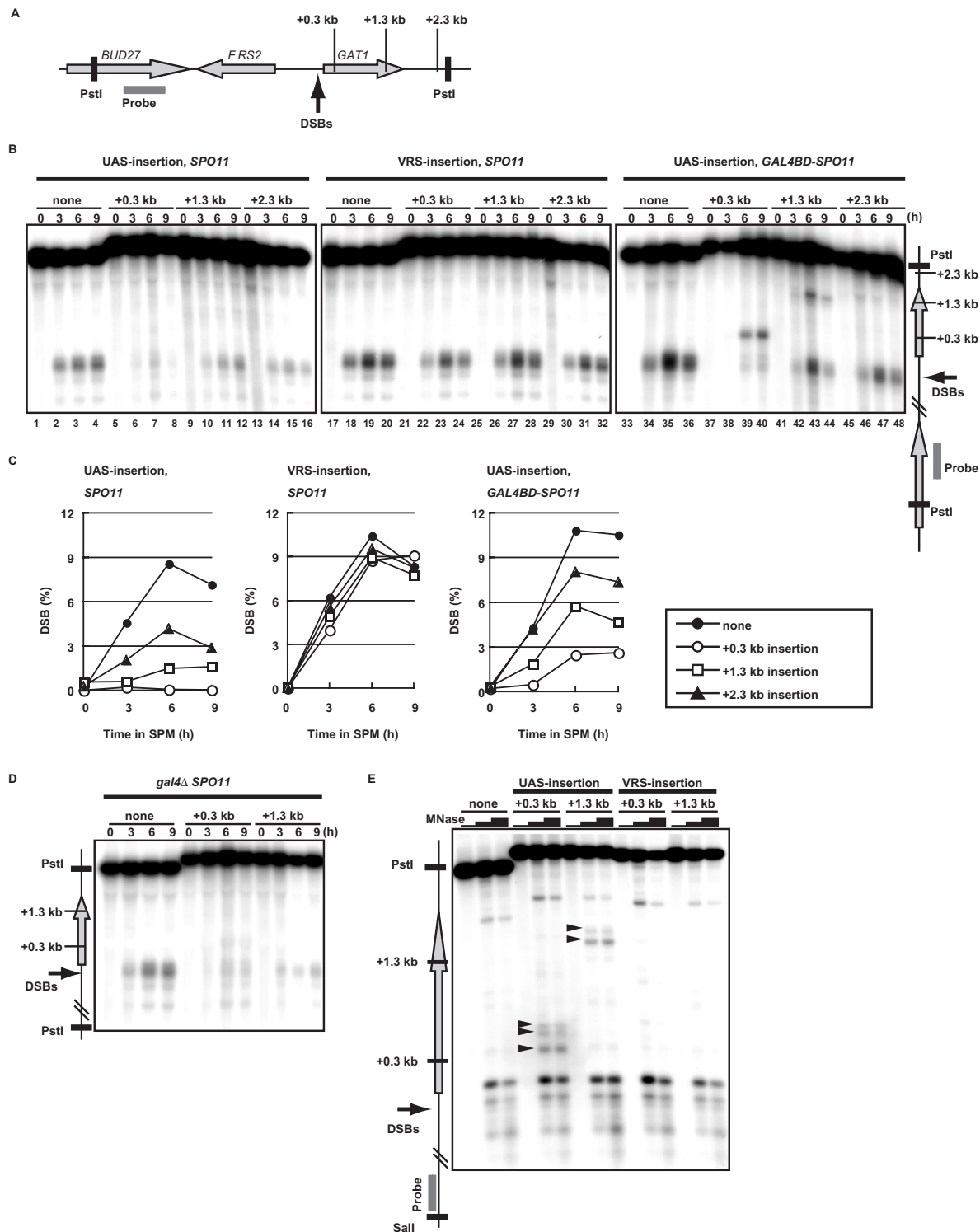


Figure 5. Repression of DSBs at the *GATI* hotspot by UAS integration. **(A)** Schematic representation of the *GATI* hotspot region. The gray arrows indicate the position and orientation of the coding region for each gene. The positions of *Pst*I sites and a probe for detection of DSBs and UAS or VRS integration sites are indicated. **(B)** Detection of *GATI* hotspot activity by Southern blot analysis. UAS (left and right panel) or VRS (middle panel) was integrated 0.3, 1.3 or 2.3 kb away from the hotspot in strains expressing Spo11 (left and middle panel) or Gal4BD-Spo11 (right panel). DNA was purified from synchronous meiotic cells at the indicated times after incubation in SPM, digested with *Pst*I, and analyzed using the probe as shown in (A). Strains without integration are designated 'none'. All strains are *sae2Δ* background without VDE-expression. Strains are derivatives of TFY372 (lanes 1–16), TFY311 (lanes 17–32) or TFY011 (lanes 33–48). **(C)** The intensities of signals corresponding to DSBs at the *GATI* hotspot were quantified and expressed as a mean of at least three independent experiments. **(D)** Southern blot analysis was performed as in (B) on strains without (none, strain TFY431) or with integration of UAS 0.3 kb (strain TFY432) or 1.3 kb (strain TFY433) away from the *GATI* hotspot. Strains have *sae2Δ* and *gal4Δ* mutations. **(E)** Meiotic chromatin (4 h) was purified from the *SPO11* strain without integration (none, strain TFY371) or its derivatives with integration of VRS or UAS 0.3 or 1.3 kb away from the *GATI* hotspot. Each chromatin sample was treated with 0, 5 or 10 U/ml of MNase. MNase-sensitive sites were detected by indirect end labeling using a probe for the sequence adjacent to the *Sal*I site. The arrowheads show MNase-sensitive sites at the UAS insertion.

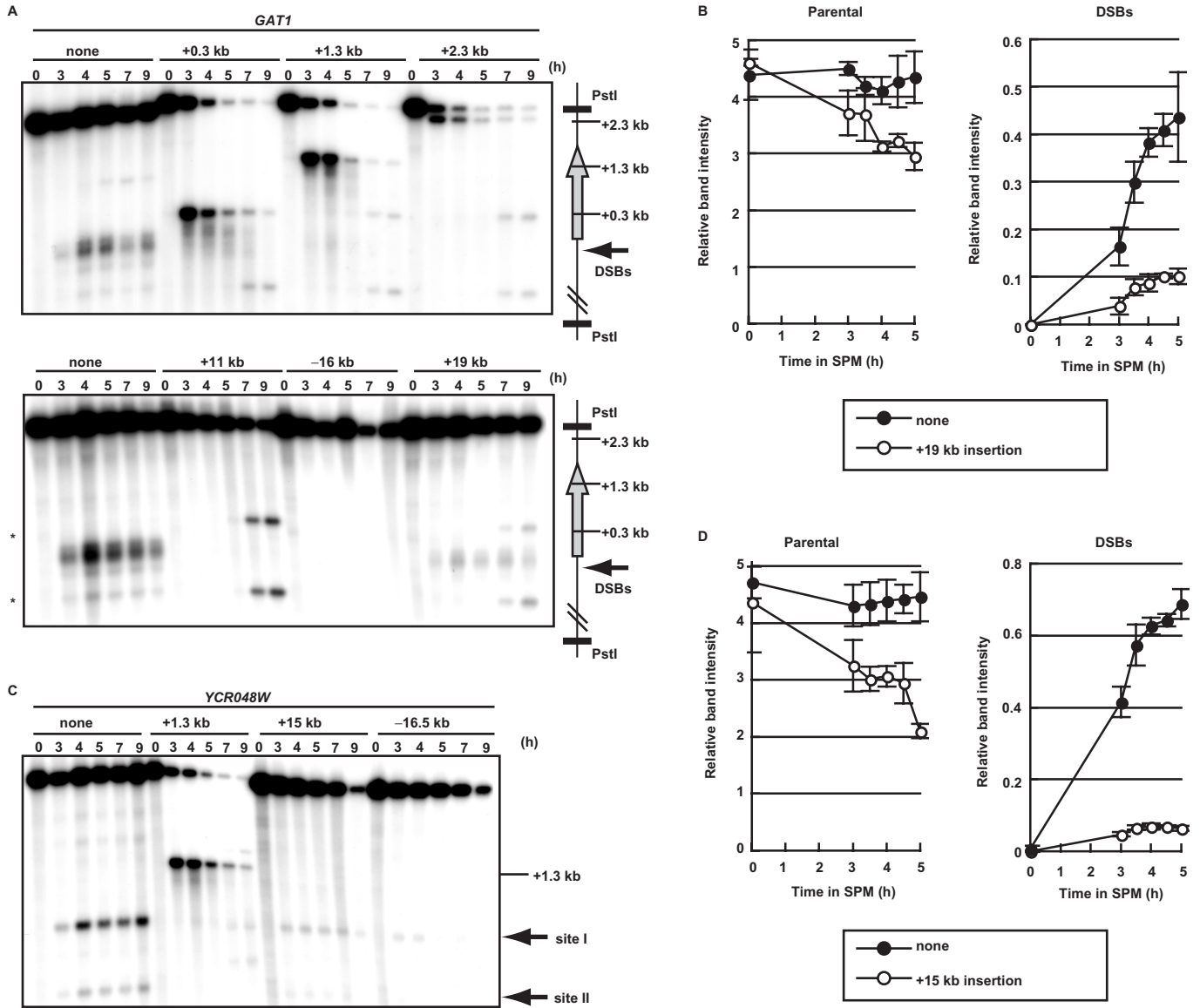


Figure 6. Repression of hotspot activity by VDE-produced DSBs. (A) VRS was integrated 0.3, 1.3, 2.3, 11 or 19-kb downstream or 16-kb upstream of the *GAT1* hotspot into the *sae2Δ* strain expressing VDE (none, strain TFY312). *GAT1* hotspot activity was examined by Southern blot analysis as in Figure 5. The asterisks indicate sites of the bands detected especially in the +11-kb insertion strain, which might stem from products formed during the repair process of VDE-introduced DSBs since the bands were detected in *spo11Δ* cells (data not shown). (B) As in (A), using VDE-expressing *sae2Δ* cells without (none) or with VRS integration 19-kb downstream of the *GAT1* hotspot (strain TFY407), the intensities of signals corresponding to parental bands (left) and DSBs at the *GAT1* hotspot (right) were determined by normalizing to an internal standard in each lane using an appropriate probe (*HIS4*). Values are expressed as a mean of three or four independent experiments with standard deviation. (C) VRS was integrated 1.3, 15 or 16 kb away from the *YCR048W* hotspot into the *sae2Δ* strain expressing VDE (none, strain TFY312). Southern blot analysis was performed as described for Figure 4. (D) As in (C), using VDE-expressing *sae2Δ* cells without (none) or with VRS integration 15 kb away from the *YCR048W* hotspot (strain TFY408), the intensities of signals corresponding to parental bands (left) and DSBs at the *YCR048W* hotspot (site I, right) were determined as described in (B). Values are expressed as a mean of four independent experiments with standard deviation.

activation of DSB among candidate sites and inhibitory effect to candidate sites by a neighboring DSB. Moreover, the latter regulation appears to contain a fully inhibitory *cis* effect and a partial *trans* effect.

DISCUSSION

In this report, we studied the effects of targeted meiotic DSB formation induced by Gal4BD-Spo11 and VDE in

order to obtain insights into regulation of the distribution of meiotic DSBs. The PCR-based method enables us to easily introduce single or multiple integrations of a sequence containing the VDE-cutting site (VRS) or containing four Gal4-binding sites (UAS) into the yeast genome using a fixed set of oligonucleotide primers. Introduction of UAS leads to an open chromatin structure at the insertion site (Figures 1C and 5E), creating a potential site for meiotic DSB formation. Indeed, DSBs

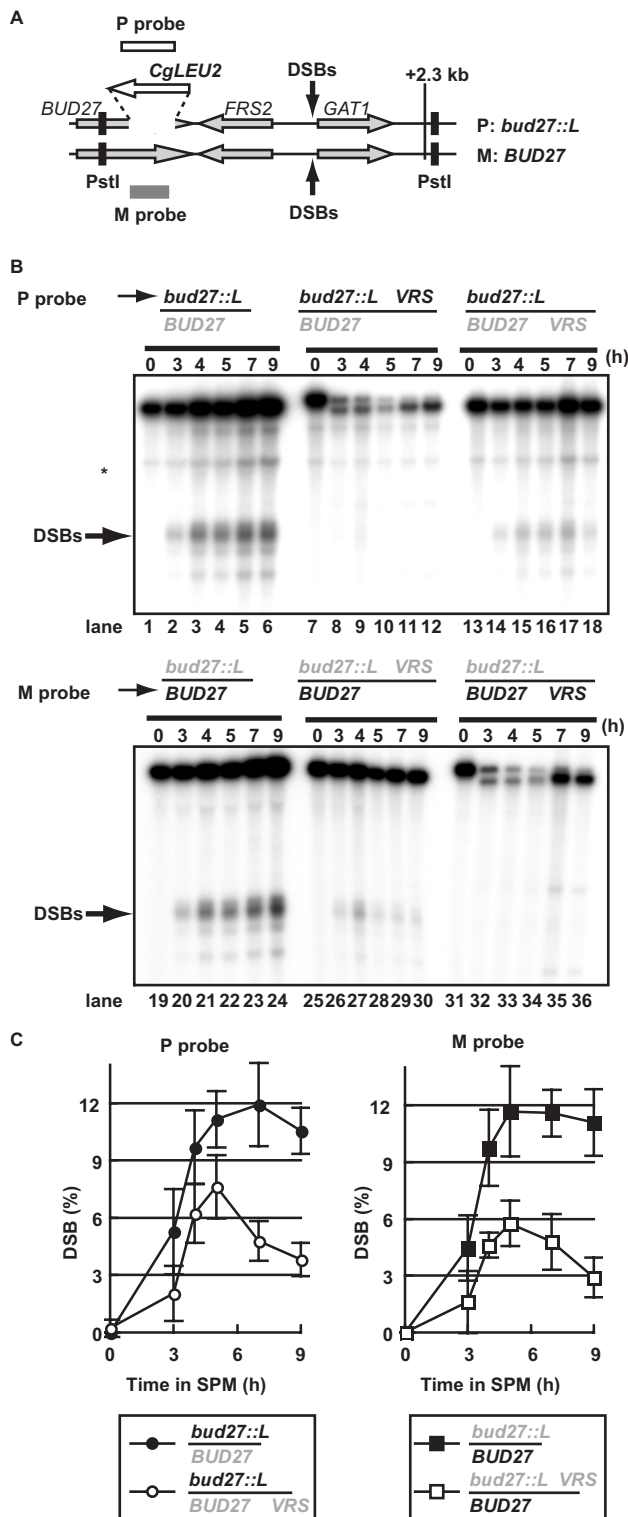


Figure 7. *Cis* and *trans* effects of VDE-mediated DSBs on hotspot activity. (A) Schematic representation of the *GAT1* hotspot region in the *BUD27/bud27::L* heterozygous diploid strain. Part of the *BUD27* gene is replaced by the *CgLEU2* gene on one homologous chromosome (P) of the diploid strain but not on the other (M). A probe specific to *CgLEU2* (P probe) and a part of *BUD27* corresponding to the deletion in P (M probe) can be used to detect the homologous chromosomes P and M, respectively. (B) VRS was introduced 2.3 kb away from *GAT1* hotspot on either the P chromosome (*bud27::L* VRS) or the M

did occur at some inserted UASs even in the *SPO11* strain, although the frequency was lower than in the *GAL4BD-SPO11* strain (Figures 2D and 4A). Here, we used these genetic tools to systematically study the effects of inducing site-specific DSBs at or around integrations sites according to the location, number, activity and manner of cleavage.

Systematic integrations of UAS along chromosome III revealed that DSBs tend to be introduced at UAS when it is inserted in a hot domain but rarely occur when it is inserted in a cold domain. This kind of domain effect has been reported by others using chromosome-wide insertion of sequence from the *ARG4* hotspot (11,21) or genome-wide comparison of binding sites and cleavage sites of Gal4BD-Spo11 (25). Furthermore, it has been revealed that insertion of Gal4-binding site near centromere III allows binding of Gal4BD-Spo11 but prevents DSB formation at the site due to an inhibitory effect by the centromere (25). Here, we also demonstrated that a cold domain is not a region of inaccessible or uncleavable chromosome structure (Figure 3). This is consistent with the previous result that cold and hot domains are similarly accessible to DNase I and topoisomerase II (21). Moreover, self-association of Spo11 does not occur at UAS in a cold domain (Figure 3D). The data suggest that not all Spo11 localized to a chromosome self-assembles and furthermore that self-interaction of Spo11 is likely to be regulated in a chromosome-domain-dependent manner. Thus, we propose that the domain effect of meiotic DSBs is regulated through activation of Spo11 in hot domains or through inhibition of Spo11 in cold domains. In addition to Spo11, at least nine other proteins have been implicated in meiotic DSB formation in *S. cerevisiae*. These proteins are thought to form a large complex consisting of multiple sub-complexes that localize to chromatin (46,47). Among them, Rec102 and Rec104 are required for self-interaction of Spo11 (35). Rec114 is dispensable for Spo11 self-interaction, but is required for meiotic loading of Spo11 to DSB sites (4,35). Therefore, it may be that the local distribution or activation of one or more of these proteins along chromosomes determines sites of DSB via promotion of Spo11 self-assembly on the chromatin.

In addition to studying the domain effect along a chromosome, we also analyzed competitive interactions among hotspots. Introductions of UAS in the vicinity of well-known hotspots revealed two types of effects. One was observed at *YCR048W* (Figure 4) and *CYS3* (Figure S2 in the Supplementary Data) and the other was observed at *GAT1* (Figure 5). The former case is consistent with the model of competition for DSB

chromosome (*BUD27* VRS) of the *BUD27/bud27::L* heterozygous diploid strain. Southern blot analysis was done using the P or M probe to detect each homologous chromosome (upper panel, P chromosome; lower panel, M chromosome). The asterisk indicates a site of cross-hybridization with the P probe, which might be attributable to the authentic *LEU2* gene locus. All strains are *sae2Δ* background expressing VDE. Lanes 1–6 and 19–24, strain TFY062; lanes 7–12 and 25–30, strain TFY063; lanes 13–18 and 31–36, strain TFY064. (C) Quantification of results obtained in (B). The intensities of signals corresponding to DSBs at the *GAT1* hotspot were quantified and expressed as a mean of four independent experiments with standard deviation.

among hotspots, in that the production of a new hotspot reduces DSB activity at nearby pre-existing hotspots, keeping the overall level of DSBs constant. Previously, mutual inhibition among hotspots has been revealed to occur both over a short range (11,12,16,24) and a long range (11,25,48). Here, we revealed that the extent of repression is higher when DSB activity is stronger at a given site. In the case of *GAT1*, an UAS insertion at *GAT1* in the *SPO11* strain reduces hotspot activity despite the fact that DSBs are not formed at the inserted UAS. This case can also be explained by competition. That is, insertion of UAS provides a potential site for meiotic DSB and then competition between the authentic hotspot and the UAS takes place, resulting in a lack of sufficient activation of DSB at either site. A similar type of repression has been reported previously: insertion of 12 tandem repeats of a nucleosome-excluding sequence generates a strong DSB hotspot, whereas insertion of 48 copies does not (49).

It is conceivable that competitive interaction among hotspots can be attributed to competition for limiting factor(s) involved in DSB formation. Spo11 is not likely to be the sole candidate for such a limiting factor, since Spo11 is abundant during meiosis and only a small fraction of the available Spo11 forms intermediate products during the formation of DSBs (50). Moreover, a mutant allele of *SPO11* defective in DSB formation does not lead to a strong dominant negative phenotype in combination with a wild-type allele, as might be expected if Spo11 were the limiting factor (26). Therefore, other component(s) of the DSB formation complex may be titrated out in a certain chromosomal regions, such that competition among DSB hotspots takes place. Alternatively, it might be that the DSB formation complex is very large or forms a specialized DNA or chromosome structure, for example, a highly bended or distorted configuration, such that the presence of a complex at one site makes it difficult or impossible for another complex to be formed nearby. If the complex generates such a specialized chromosome structure, it would be possible that meiotic chromatin transition observed at active DSB sites reflects such a specialized structure (14,37).

Intriguingly, DNA cleavage by VDE represses DSB formation over a region of ~20 kb in length (Figure 6), implicating formed DSB itself in interactions among hotspots. DSB formation by VDE apparently occurs via a pathway parallel to that mediated by Spo11, since VDE can cleave its target in the absence of the Spo11 DSB formation complex (30) and without regard to the chromosomal context of its target (Figure 3B). Hence, in addition to competition for factors involved in DSB formation, it is likely that there is also a mechanism for restricting the number of DSBs that recognizes a DSB at one site and transmits the signal to prevent DSB formation at neighboring other potential sites. Several studies on mitotic cells suffering a DSB have revealed that after cleavage, DSB ends are subjected to multiple interdependent or independent processes, including DNA end resection, chromatin remodeling, histone modification and recruitment of repair proteins or cohesin

complex (51). It is currently not known if these are relevant to meiotic cells, however, it seems reasonable that one or more of these processes might affect the DSB formation machinery and inhibit Spo11-mediated DSBs near an existing cleavage site. For example, it is conceivable that resection of DSB ends removes the DSB formation complex from DNA. Alternatively, DSB-induced nucleosome remodeling or histone modification may alter the chromatin configuration or histone code required for DSB formation (9,52–54). A further possibility is that loading of the cohesin complex onto DSB sites may help to recruit the DNA region into the chromosome axis, where DSBs rarely occur. Indeed, phosphorylation of histone H2A (55) or loading of cohesin (56,57) has been observed to occur over a large region (~50 kb) surrounding a DSB, a region sufficient in size to explain DSB repression by VDE observed in our study. It is also possible that DSB repair proteins loaded around the DSB site inactivate or replace the DSB formation complex. Some repair proteins can invade or capture a homologous chromatid as well as a broken chromatid, explaining the *trans* inhibition of DSBs observed at an intact homologous chromosome (Figure 7). In addition to these factors, which act upon DSB ends directly, we should consider the possibility of mechanical or physical aspects of DNA caused by DSB as discussed in crossover controls (58,59). For example, it might be that DSB formation at a site alters the mechanical forces on DNA that are a prerequisite for DSB formation by Spo11, such as alteration in regional DNA topology, an increase or decrease in mechanical stress or release of a tension. These mechanical or physical factors may help to explain the highly rapid and locus-specific suppression of DSBs in a region already containing a break.

The domain effect restricts the positioning of DSBs within particular hot domains and the interaction among hotspots limits the number of DSBs. During meiotic recombination, crossover interference and crossover homeostasis tightly regulate the distribution of crossovers (59,60). To ensure that DSBs are sufficiently abundant also seems important, since mutant strains that produce fewer DSBs also have reduced viability during meiosis (26). On the other hand, excess production of DSBs should also be avoided, since DSBs are deleterious lesions that can cause genomic instability and dose-dependent cell death. Therefore, ensuring and limiting the number of DSB seems an essential point of regulation for cell integrity. Furthermore, the location of DSBs also seems important, since formation of a chiasma at an inappropriate site can lead to chromosome missegregation (27). Thus, the molecular mechanisms and physiological significance of the distribution of meiotic DSBs remain issues of importance. VDE, which can cause a DSB even in a cold domain, may be a useful tool for uncovering novel insights into these issues. VDE can potentially make it possible to completely re-program the number and location of DSBs in a *spo11* background via designed insertions of VRS, such that we could systematically study how changes in the distribution of DSBs affect the behaviors of meiotic chromosomes.

SUPPLEMENTARY DATA

Supplementary Data are available at NAR Online.

ACKNOWLEDGEMENTS

We are grateful to A. Nicolas and Y. Ohya for providing materials used in this study. We thank Y. Hosono-Sakuma for technical assistance. This work was supported by grants for basic research from the Bio-oriented Technology Research Advancement Institution to K.O. and T.S. and a grant-in-aid for scientific research on priority areas from the Ministry of Education, Culture, Sports, Science, and Technology of Japan. This work was also assisted by a grant-in-aid for scientific research from the Japan Society for the Promotion of Science and the RIKEN Special Postdoctoral Researchers Program to T.F. Funding to pay the Open Access publication charges for this article was provided by the grants listed above.

Conflict of interest statement. None declared.

REFERENCES

- Petronczki, M., Siomos, M.F. and Nasmyth, K. (2003) Un ménage à quatre: the molecular biology of chromosome segregation in meiosis. *Cell*, **112**, 423–440.
- Keeney, S. (2001) Mechanism and control of meiotic recombination initiation. *Curr. Top. Dev. Biol.*, **52**, 1–53.
- Libby, B.J., Reinholdt, L.G. and Schimenti, J.C. (2003) Positional cloning and characterization of Mei1, a vertebrate-specific gene required for normal meiotic chromosome synapsis in mice. *Proc. Natl Acad. Sci. USA*, **100**, 15706–15711.
- Prieler, S., Penkner, A., Borde, V. and Klein, F. (2005) The control of Spo11's interaction with meiotic recombination hotspots. *Genes Dev.*, **19**, 255–269.
- De Muyt, A., Vezon, D., Gendrot, G., Gallois, J.L., Stevens, R. and Grelon, M. (2007) AtPRD1 is required for meiotic double strand break formation in *Arabidopsis thaliana*. *EMBO J.*, **26**, 4126–4137.
- Petes, T.D. (2001) Meiotic recombination hot spots and cold spots. *Nat. Rev. Genet.*, **2**, 360–369.
- Haring, S.J., Lautner, L.J., Comeron, J.M. and Malone, R.E. (2004) A test of the CoHR motif associated with meiotic double-strand breaks in *Saccharomyces cerevisiae*. *EMBO Rep.*, **5**, 41–46.
- Kirkpatrick, D.T., Fan, Q. and Petes, T.D. (1999) Maximal stimulation of meiotic recombination by a yeast transcription factor requires the transcription activation domain and a DNA-binding domain. *Genetics*, **152**, 101–115.
- Yamada, T., Mizuno, K., Hirota, K., Kon, N., Wahls, W.P., Hartsuiker, E., Murofushi, H., Shibata, T. and Ohta, K. (2004) Roles of histone acetylation and chromatin remodeling factor in a meiotic recombination hotspot. *EMBO J.*, **23**, 1792–1803.
- Cao, L., Alani, E. and Kleckner, N. (1990) A pathway for generation and processing of double-strand breaks during meiotic recombination in *S. cerevisiae*. *Cell*, **61**, 1089–1101.
- Wu, T.C. and Lichten, M. (1995) Factors that affect the location and frequency of meiosis-induced double-strand breaks in *Saccharomyces cerevisiae*. *Genetics*, **140**, 55–66.
- Fan, Q.Q., Xu, F., White, M.A. and Petes, T.D. (1997) Competition between adjacent meiotic recombination hotspots in the yeast *Saccharomyces cerevisiae*. *Genetics*, **145**, 661–670.
- Wu, T.C. and Lichten, M. (1994) Meiosis-induced double-strand break sites determined by yeast chromatin structure. *Science*, **263**, 515–518.
- Ohta, K., Shibata, T. and Nicolas, A. (1994) Changes in chromatin structure at recombination initiation sites during yeast meiosis. *EMBO J.*, **13**, 5754–5763.
- Mizuno, K., Emura, Y., Baur, M., Kohli, J., Ohta, K. and Shibata, T. (1997) The meiotic recombination hot spot created by the single-base substitution *ade6-M26* results in remodeling of chromatin structure in fission yeast. *Genes Dev.*, **11**, 876–886.
- Xu, L. and Kleckner, N. (1995) Sequence non-specific double-strand breaks and interhomolog interactions prior to double-strand break formation at a meiotic recombination hot spot in yeast. *EMBO J.*, **14**, 5115–5128.
- Glynn, E.F., Megee, P.C., Yu, H.G., Mistrot, C., Unal, E., Koshland, D.E., DeRisi, J.L. and Gerton, J.L. (2004) Genome-wide mapping of the cohesin complex in the yeast *Saccharomyces cerevisiae*. *PLoS Biol.*, **2**, E259.
- Blat, Y., Protacio, R.U., Hunter, N. and Kleckner, N. (2002) Physical and functional interactions among basic chromosome organizational features govern early steps of meiotic chiasma formation. *Cell*, **111**, 791–802.
- Baudat, F. and Nicolas, A. (1997) Clustering of meiotic double-strand breaks on yeast chromosome III. *Proc. Natl Acad. Sci. USA*, **94**, 5213–5218.
- Gerton, J.L., DeRisi, J., Shroff, R., Lichten, M., Brown, P.O. and Petes, T.D. (2000) Inaugural article: global mapping of meiotic recombination hotspots and coldspots in the yeast *Saccharomyces cerevisiae*. *Proc. Natl Acad. Sci. USA*, **97**, 11383–11390.
- Borde, V., Wu, T.C. and Lichten, M. (1999) Use of a recombination reporter insert to define meiotic recombination domains on chromosome III of *Saccharomyces cerevisiae*. *Mol. Cell. Biol.*, **19**, 4832–4842.
- Petes, T.D. and Merker, J.D. (2002) Context dependence of meiotic recombination hotspots in yeast: the relationship between recombination activity of a reporter construct and base composition. *Genetics*, **162**, 2049–2052.
- Borde, V., Goldman, A.S. and Lichten, M. (2000) Direct coupling between meiotic DNA replication and recombination initiation. *Science*, **290**, 806–809.
- Pecina, A., Smith, K.N., Mezard, C., Murakami, H., Ohta, K. and Nicolas, A. (2002) Targeted stimulation of meiotic recombination. *Cell*, **111**, 173–184.
- Robine, N., Uematsu, N., Amiot, F., Gidrol, X., Barillot, E., Nicolas, A. and Borde, V. (2007) Genome-wide redistribution of meiotic double-strand breaks in *Saccharomyces cerevisiae*. *Mol. Cell. Biol.*, **27**, 1868–1880.
- Diaz, R.L., Alcid, A.D., Berger, J.M. and Keeney, S. (2002) Identification of residues in yeast Spo11p critical for meiotic DNA double-strand break formation. *Mol. Cell. Biol.*, **22**, 1106–1115.
- Rockmill, B., Voelkel-Meiman, K. and Roeder, G.S. (2006) Centromere-proximal crossovers are associated with precocious separation of sister chromatids during meiosis in *Saccharomyces cerevisiae*. *Genetics*, **174**, 1745–1754.
- Ross, L.O., Maxfield, R. and Dawson, D. (1996) Exchanges are not equally able to enhance meiotic chromosome segregation in yeast. *Proc. Natl Acad. Sci. USA*, **93**, 4979–4983.
- Gimble, F.S. and Thorner, J. (1992) Homing of a DNA endonuclease gene by meiotic gene conversion in *Saccharomyces cerevisiae*. *Nature*, **357**, 301–306.
- Fukuda, T., Nogami, S. and Ohya, Y. (2003) VDE-initiated intein homing in *Saccharomyces cerevisiae* proceeds in a meiotic recombination-like manner. *Genes Cells*, **8**, 587–602.
- Kane, S.M. and Roth, R. (1974) Carbohydrate metabolism during ascospore development in yeast. *J. Bacteriol.*, **118**, 8–14.
- Adams, A., Gottschling, D., Kaiser, C. and Stearns, T. (1997) *Methods in Yeast Genetics*, Cold Spring Harbor Laboratory Press, New York.
- Nogami, S., Fukuda, T., Nagai, Y., Yabe, S., Sugiura, M., Mizutani, R., Satow, Y., Anraku, Y. and Ohya, Y. (2002) Homing at an extragenic locus mediated by VDE (PI-SceI) in *Saccharomyces cerevisiae*. *Yeast*, **19**, 773–782.
- Fukuda, T., Ohya, Y. and Ohta, K. (2007) Conditional genomic rearrangement by designed meiotic recombination using VDE (PI-SceI) in yeast. *Mol. Genet. Genomics*, **278**, 467–478.
- Sasanuma, H., Murakami, H., Fukuda, T., Shibata, T., Nicolas, A. and Ohta, K. (2007) Meiotic association between Spo11 regulated by Rec102, Rec104 and Rec114. *Nucleic Acids Res.*, **35**, 1119–1133.
- Sakumoto, N., Mukai, Y., Uchida, K., Kouchi, T., Kuwajima, J., Nakagawa, Y., Sugioka, S., Yamamoto, E., Furuyama, T. et al. (1999)

- A series of protein phosphatase gene disruptants in *Saccharomyces cerevisiae*. *Yeast*, **15**, 1669–1679.
37. Ohta, K., Nicolas, A., Furuse, M., Nabetani, A., Ogawa, H. and Shibata, T. (1998) Mutations in the *MRE11*, *RAD50*, *XRS2*, and *MRE2* genes alter chromatin configuration at meiotic DNA double-stranded break sites in premeiotic and meiotic cells. *Proc. Natl Acad. Sci. USA*, **95**, 646–651.
 38. Fukuda, T., Ohta, K. and Ohya, Y. (2006) Investigation of the mechanism of meiotic DNA cleavage by *VMA1*-derived endonuclease uncovers a meiotic alteration in chromatin structure around the target site. *Eukaryot. Cell*, **5**, 981–990.
 39. Church, G.M. and Gilbert, W. (1984) Genomic sequencing. *Proc. Natl Acad. Sci. USA*, **81**, 1991–1995.
 40. Prinz, S., Amon, A. and Klein, F. (1997) Isolation of *COM1*, a new gene required to complete meiotic double-strand break-induced recombination in *Saccharomyces cerevisiae*. *Genetics*, **146**, 781–795.
 41. McKee, A.H. and Kleckner, N. (1997) A general method for identifying recessive diploid-specific mutations in *Saccharomyces cerevisiae*, its application to the isolation of mutants blocked at intermediate stages of meiotic prophase and characterization of a new gene *SAE2*. *Genetics*, **146**, 797–816.
 42. Ohta, K., Wu, T.C., Lichten, M. and Shibata, T. (1999) Competitive inactivation of a double-strand DNA break site involves parallel suppression of meiosis-induced changes in chromatin configuration. *Nucleic Acids Res.*, **27**, 2175–2180.
 43. Smith, A.V. and Roeder, G.S. (1997) The yeast Red1 protein localizes to the cores of meiotic chromosomes. *J. Cell. Biol.*, **136**, 957–967.
 44. Klein, F., Mahr, P., Galova, M., Buonomo, S.B., Michaelis, C., Nairz, K. and Nasmyth, K. (1999) A central role for cohesins in sister chromatid cohesion, formation of axial elements, and recombination during yeast meiosis. *Cell*, **98**, 91–103.
 45. Haring, S.J., Halley, G.R., Jones, A.J. and Malone, R.E. (2003) Properties of natural double-strand-break sites at a recombination hotspot in *Saccharomyces cerevisiae*. *Genetics*, **165**, 101–114.
 46. Arora, C., Kee, K., Maleki, S. and Keeney, S. (2004) Antiviral protein Ski8 is a direct partner of Spo11 in meiotic DNA break formation, independent of its cytoplasmic role in RNA metabolism. *Mol. Cell*, **13**, 549–559.
 47. Maleki, S., Neale, M.J., Arora, C., Henderson, K.A. and Keeney, S. (2007) Interactions between Mei4, Rec114, and other proteins required for meiotic DNA double-strand break formation in *Saccharomyces cerevisiae*. *Chromosoma*, **116**, 471–486.
 48. Jessop, L., Allers, T. and Lichten, M. (2005) Infrequent co-conversion of markers flanking a meiotic recombination initiation site in *Saccharomyces cerevisiae*. *Genetics*, **169**, 1353–1367.
 49. Kirkpatrick, D.T., Wang, Y.H., Dominska, M., Griffith, J.D. and Petes, T.D. (1999) Control of meiotic recombination and gene expression in yeast by a simple repetitive DNA sequence that excludes nucleosomes. *Mol. Cell. Biol.*, **19**, 7661–7671.
 50. Neale, M.J., Pan, J. and Keeney, S. (2005) Endonucleolytic processing of covalent protein-linked DNA double-strand breaks. *Nature*, **436**, 1053–1057.
 51. Bao, Y. and Shen, X. (2007) Chromatin remodeling in DNA double-strand break repair. *Curr. Opin. Genet. Dev.*, **17**, 126–131.
 52. Sollier, J., Lin, W., Soustelle, C., Suhre, K., Nicolas, A., Geli, V. and de La Roche Saint-Andre, C. (2004) Set1 is required for meiotic S-phase onset, double-strand break formation and middle gene expression. *EMBO J.*, **23**, 1957–1967.
 53. Yamashita, K., Shinohara, M. and Shinohara, A. (2004) Rad6-Bre1-mediated histone H2B ubiquitylation modulates the formation of double-strand breaks during meiosis. *Proc. Natl Acad. Sci. USA*, **101**, 11380–11385.
 54. Mieczkowski, P.A., Dominska, M., Buck, M.J., Lieb, J.D. and Petes, T.D. (2007) Loss of a histone deacetylase dramatically alters the genomic distribution of Spo11p-catalyzed DNA breaks in *Saccharomyces cerevisiae*. *Proc. Natl Acad. Sci. USA*, **104**, 3955–3960.
 55. Shroff, R., Arbel-Eden, A., Pilch, D., Ira, G., Bonner, W.M., Petrini, J.H., Haber, J.E. and Lichten, M. (2004) Distribution and dynamics of chromatin modification induced by a defined DNA double-strand break. *Curr. Biol.*, **14**, 1703–1711.
 56. Unal, E., Arbel-Eden, A., Sattler, U., Shroff, R., Lichten, M., Haber, J.E. and Koshland, D. (2004) DNA damage response pathway uses histone modification to assemble a double-strand break-specific cohesin domain. *Mol. Cell*, **16**, 991–1002.
 57. Strom, L., Lindroos, H.B., Shirahige, K. and Sjogren, C. (2004) Postreplicative recruitment of cohesin to double-strand breaks is required for DNA repair. *Mol. Cell*, **16**, 1003–1015.
 58. Kleckner, N., Zickler, D., Jones, G.H., Dekker, J., Padmore, R., Henle, J. and Hutchinson, J. (2004) A mechanical basis for chromosome function. *Proc. Natl Acad. Sci. USA*, **101**, 12592–12597.
 59. Martini, E., Diaz, R.L., Hunter, N. and Keeney, S. (2006) Crossover homeostasis in yeast meiosis. *Cell*, **126**, 285–295.
 60. Hillers, K.J. (2004) Crossover interference. *Curr. Biol.*, **14**, R1036–R1037.